The cold regions hydrological model: a platform for basing process representation and model structure on physical evidence

J. W. Pomeroy,[1]* D. M. Gray,[1†] T. Brown,[1] N. R. Hedstrom,[2] W. L. Quinton,[3] R. J. Granger[2] and S. K. Carey[4]

[1] *Centre for Hydrology, University of Saskatchewan, 117 Science Place, Saskatoon, Saskatchewan, S7N 5C8, Canada*
[2] *National Water Research Institute, Environment Canada, 11 Innovation Boulevard, Saskatoon, Saskatchewan, Canada*
[3] *Cold Regions Research Centre, Wilfrid Laurier University, Waterloo, Ontario, Canada*
[4] *Department of Geography and Environmental Studies, Carleton University, Ottawa, Ontario, Canada*

Abstract:

After a programme of integrated field and modelling research, hydrological processes of considerable uncertainty such as snow redistribution by wind, snow interception, sublimation, snowmelt, infiltration into frozen soils, hillslope water movement over permafrost, actual evaporation, and radiation exchange to complex surfaces have been described using physically based algorithms. The cold regions hydrological model (CRHM) platform, a flexible object-oriented modelling system was devised to incorporate these algorithms and others and to connect them for purposes of simulating the cold regions hydrological cycle over small to medium sized basins. Landscape elements in CRHM can be linked episodically in process-specific cascades via blowing snow transport, overland flow, organic layer subsurface flow, mineral interflow, groundwater flow, and streamflow. CRHM has a simple user interface but no provision for calibration; parameters and model structure are selected based on the understanding of the hydrological system; as such the model can be used both for prediction and for diagnosis of the adequacy of hydrological understanding. The model is described and demonstrated in basins from the semi-arid prairie to boreal forest, mountain and muskeg regions of Canada where traditional hydrological models have great difficulty in describing hydrological phenomena. Some success is shown in simulating various elements of the hydrological cycle without calibration; this is encouraging for predicting hydrology in ungauged basins. Copyright © 2007 John Wiley & Sons, Ltd.

KEY WORDS   hydrological modelling; blowing snow; snowmelt; frozen soil infiltration; evaporation; subsurface flow; hillslope runoff; hydrological response unit; distributed modelling; physically based modelling

Received 1 June 2006; Accepted 12 December 2006

INTRODUCTION

A coupled field investigation and modelling programme has been in operation in western and northern Canada for several decades. The programme has focussed on improving the understanding, description, and simulation of hydrological processes that are relevant to the cold continental climate in Canada, in the central and western provinces and northern territories and including prairie, parkland, boreal forest, subarctic, arctic and high elevation forest, and tundra environments. These regions are currently undergoing increased agricultural, forestry, and mining development and are subject to climate warming (Serreze *et al.*, 2000). Similar hydrometeorological regimes, whilst widespread in the world, are usually found in sparsely populated, poorly gauged, regions. For example, their character and approach to modelling in Russia has been described by

Kuchment *et al.* (1983, 2000) and in Alaska by Zhang *et al.* (2000) and Bowling *et al.* (2004). The hydrology of cold regions in Canada is characterized by low to moderate precipitation inputs, cold winters, and substantive water storage by the seasonal snowcover, seasonally or perennially frozen ground, glacial geomorphology resulting in poorly defined drainage, highly episodic runoff events, and strong linkage between the mass balance and the energy balance through phase changes. Early in the experimental programme it was observed that:

1. the spring snowmelt freshet was normally the largest runoff event of the year and was followed by much smaller summer flows (Gray, 1970),
2. large changes in snow accumulation did not always correspond to large changes in the magnitude of the spring freshet; rather the freshet was also highly sensitive to antecedent soil moisture and ground ice conditions (Gray and Granger, 1986),
3. the impact of heavy rainfall on summer flows was highly variable and often modest, except for the effect of intensive convective rainfall (Gray, 1970).

* Correspondence to: J. W. Pomeroy, Centre for Hydrology, University of Saskatchewan, 117 Science Place, Saskatoon, Saskatchewan, S7N 5C8, Canada. E-mail: pomeroy@usask.ca
† Professor Gray sadly passed away during the preparation of this manuscript.

As such, the classical concepts of rainfall-runoff response in these basins could not be used to describe their hydrological behaviour.

Particular problems were identified in understanding and calculation of the following processes that were felt to be responsible for this basin behaviour:

1. snow redistribution by wind and vegetation (e.g. Pomeroy *et al.*, 1993; Pomeroy *et al.*, 1998)
2. snowmelt (e.g. Male and Gray, 1981)
3. infiltration to unsaturated frozen soils, including cracked soils (e.g. Granger *et al.*, 1984)
4. evaporation from unsaturated surfaces (e.g. Granger and Gray, 1989)
5. hillslope water redistribution over frozen ground (e.g. Quinton and Marsh, 1998).

To develop an improved understanding of these processes required very specific and novel process observation strategies. To apply them to these basins required an understanding of their variability over space and sensitivity to boundary and initial conditions.

An urgent need in hydrology is to apply models to predict in ungauged basins and hence traditional calibration of models is not possible (Sivapalan *et al.*, 2003). A purpose-built physically based model based on a good understanding of the principles and characteristics of hydrology in a basin, with an appropriate structure and appropriate spatial resolution and parameter selection, should have a good chance of simulating the hydrological cycle including the water balance, streamflow, and other variables of interest such as soil moisture and snow accumulation. Logical selection and design of model strategy, structure, and their inherent assumptions are governed by local problems and local hydrology—this is not just parameter selection but involves selection of an appropriate model structure.

This paper describes how physically-based algorithms describing various hydrological processes were linked into a new modelling system that has resulted in the physically-based spatially-distributed cold regions hydrological model (CRHM). The model's features, functions, and structure are described. It will then demonstrate, using examples, how CRHM has proven to be a potentially useful research tool in diagnosing the hydrological cycle and in predicting elements of this cycle in the Canadian cold regions where calibration against measured streamflow is not possible or warranted.

COLD REGIONS HYDROLOGICAL MODEL OVERVIEW

CRHM is a modular model that permits appropriate hydrological processes for the basin, selected from a library of process modules, to be linked to simulate the hydrological cycle of hydrological response units (HRUs). HRU are defined here as spatial units of mass and energy balance calculation that correspond to biophysical landscape units, within which processes and states can be adequately described for the calculation by single sets of parameters, state variables, and fluxes including horizontal fluxes *but having a place in a landscape sequence or water/snow cascade*. HRU have biophysical states such as vegetation cover, state variables such as soil moisture, and fluxes in vertical and horizontal directions such as evaporation and runoff. HRU need not include a stream channel and may be as fine scaled as hillslope segments or as coarse-scaled as a sub-basin. Typically, HRU correspond to the forest stand, agricultural field, hillslope, or valley bottom scale. CRHM routes the water between the HRU via varying pathways, such as blowing snow transport, overland flow, organic subsurface flow, mineral interflow, groundwater flow, and streamflow when some threshold condition (wind speed, soil moisture content, infiltration excess, etc) is exceeded or using a conductivity-gradient approach. The flow direction and sequences between HRU can be specific to the process and pathways; for instance, blowing snow is routed from low vegetation to high vegetation HRU, subsurface flow is routed downslope and streamflow is routed according to the stream network. So the flow sequence between HRU can vary with the flow process—this permits characterization of a basin as a series of HRU cascades.

Because there is a high level of confidence in the process representations of the modules and good flexibility of model structure, there is diminished need for calibration for discharge simulations. Calibration can often be restricted to streamflow routing and baseflow aspects of the model or omitted completely. It is felt that models that have been forced to represent the process operation and outputs faithfully will have more robust application and diminished routing parameter estimation uncertainty.

CRHM uses a modular modelling object-oriented structure (Leavesley *et al.*, 1996) to develop, support, and apply dynamic model routines. The integrated system of software provides the framework to develop and evaluate physically-based algorithms and effectively integrate selected algorithms into a model. Existing algorithms can be modified or new algorithms can be developed and added as modules to the module library. Modules from the library are coupled to create a purpose-built model, suited for the specific application. CHRM module development has focussed on specific and often neglected cold region aspects of hydrology. Each module represents a physically-based algorithm or data transformation.

The approach used in CRHM differs from many other hydrological models in that it is highly flexible and modular following Leavesley *et al.*'s (1996, 2002) concepts in the modular modelling system (MMS). CRHM differs from MMS in that it incorporates a full range of cold regions hydrological processes and employs a unique conception of cascading HRU. Cold regions hydrological processes are well represented in models such as ARHYTHM (Zhang *et al.*, 2000) and VIC (Bowling *et al.*, 2004); however CRHM has a more complete range of processes for this environment (blowing snow, intercepted snow, energy balance snowmelt, infiltration to

frozen soils, etc) and a wide range of selection in process descriptions from the conceptual to the physically-based. CRHM HRU can be placed in landscape water and snow cascades so that snow redistribution processes, and episodic drainage from poorly drained, often dry sites can be simulated appropriately. This is a more detailed spatial representation than the grouped HRU approach of Kite (1995) and Kouwen *et al.* (1993) where all HRU must route to a stream and there is no topographic position assigned to a unit (tile). However, it is less spatially detailed than the finely distributed approach employed by models such as Systeme Hydrologique Europeen (SHE) (Abbott *et al.*, 1986) because parameter availability in much of Canada is severely constrained by lack of observations and reliable inventory. Because CRHM offers flexible spatial representation from lumped to distributed approaches, it permits the selection of a suitable spatial scale for the biophysical structure and climate of the basin, for data availability, and for the purpose of the simulation. By balancing complexity and parameter uncertainty with necessary process representation and spatial resolution the model can help the researcher select the most appropriate approach and structure for simulations that minimize uncertainty. It is clear that at large scales this will be simplified (e.g. Woo and Thorne, 2006) but at small scales this must be very detailed (e.g. Quinton *et al.*, 2004).

CHRM is fundamentally different from most hydrological models because it is a modelling platform from which models can be created. It is recognized that it is inappropriate to run detailed distributed models where parameter and hydrological uncertainty are so great as to make the operation of these models physically-unrealistic. By offering a range of spatial complexity from lumped to distributed, of physical realism from the conceptual to physically based approaches and by offering a wide selection of process modules CRHM permits the user to tailor the model to the appropriate complexity that is warranted by the modelling objective, scale, and available information on the basin. The CRHM platform can be used to create many models of a basin for purposes of intercomparison, testing of new algorithms, evaluation of model structure, and estimation of predictive uncertainty.

Components of CRHM

CRHM has the following components:

1. Observations—These are time-series meteorological data and surface observations of streamflow, snowpack, or soil moisture at varying intervals.
2. Parameters—Spatial data (e.g. basin area, elevation, and cover type) are generated using a GIS interface tool to assist the user in basin delineation, characterization and parameterization of HRU. HRU are subdivisions of the basin characterized by the operator from an understanding of the hydrological processes, terrain, and land use. Parameters for HRU can also be input by the user on a screen.

3. Modules—Algorithms implementing the hydrological/physical processes are chosen by the user. The model data structure is specified by the declarations in the modules but is implemented globally by the CRHM platform.
4. Groups—A collection of modules executed in sequence for all HRUs can be linked as a Group. The Group can be used in place of specific individual modules and this is often a convenient way to characterize a complex set of processes that consistently operate in a particular environment or hydrological classification.
5. Structure—A parallel collection of modules, essentially a Group applied to specific HRU. HRU can have varying Structures. Structures can be used for comparison of sets of algorithms, and customization of model design to unique HRU characteristics. Structures permit diverse sets of modules to be representative of both the HRU and basin.
6. Variables and States—These are created by the declarations in the modules. Variables include meteorological drivers such as precipitation, temperature, wind speed and States are HRU conditions such as soil moisture, snow water equivalent, and albedo.

CRHM model platform

The CRHM Model Platform performs the following services:

Basic functions:

1. Configures the model to the number of HRU and HRU layers.
2. Builds the selected Modules, Groups or Structures into a working model after checking the structure and data flow of the model.
3. Links the Observation files to the model.
4. Links the Parameter data to the model.
5. Permits initial State files to be set up as input to the model or as output to receive the final state of the model.
6. Sets the duration of the model run.
7. Selects the desired State/Variable values to be displayed and available for output.
8. Executes the model.
9. Provides interaction with the graphical display.

Housekeeping functions:

1. Saves and loads project files to allow the model (Project) to be saved as an entirety which can be loaded and run later.
2. Helps in operating the CRHM platform and describing the functionality of the Module, Variables and States.
3. Exports the model output to files for use by other applications (e.g. Microsoft Excel).
4. Exports the model output for later input to compare with other CRHM model runs with different parameter values.

5. Provides the statistical and graphical tools to analyse input data and the model performance.
6. Models module flow diagrams to demonstrate data flow within the model. Driving Observations or input Parameters are superimposed on the flow diagram to help the user to visualize their entry into the model.
7. Maps model output onto HRU shapes to aid spatial visualization of the model results.
8. Displays observations as diagnostic tools to detect data problems. This is enhanced by the capability to plot the time series data as daily mean, daily maximum, daily minimum, daily sum, and cumulative sum. Other functions are also available.
9. Manipulates observation data using filters. These filters take various forms. Examples are scaling, unit changing, time interval changing and replacing missing or faulty data with adjacent or interpolated data.
10. Helps the user to synthesize input observation data using functions to generate sine/ramp/pulse/log etc. waveforms as a function of time. These simple driving inputs are indispensable for diagnostic testing as actual meteorological data can be too complex to initially comprehend and test algorithms.
11. Displays, edits, and saves or loads parameters from files. Two options are available. The first is from text files and the second is from database files.
12. Imports ArcGIS data as a shapefile as CRHM is compatible with ESRI® shapefile software to set parameter values and HRU and basin perimeter coordinates.

Expandable Aspects:

1. Users can create their own modules with basic knowledge of C++. These modules are linked to make an executable dynamic linked library (DLL) which is loaded into CRHM. The user written modules are handled identically to the original modules.
2. Users can create help files describing the capabilities of their custom modules and CRHM will automatically integrate the help file into the CRHM help menu.
3. Users can replace existing CRHM modules with custom versions of a module to test enhancements, simplifications or to add diagnostic variables.
4. Users can avail of a Macro facility that permits them to write their own provisional macro-module from within CRHM, using a simple logical language, and to link these macros to the rest of the model structure. Macros permit rapid experimentation with model structure and are intended for variable and parameter transformations between existing modules or for testing a potential module performance.

CRHM MODULES

The complete set of CRHM modules can be classified into the following categories; for many categories there is a choice of procedures ranging from basic to strongly physically-based, so as to permit the most appropriate algorithms to be used for the available data, information reliability, basin characteristics, scale, intended output, etc:

1. Basin: sets basin and HRU physical, soil, and vegetation characteristics;
2. Observation: interpolates meteorological data to HRU using adiabatic relationships, and saturation vapour pressure calculations;
3. Snow transport: uses blowing snow transport and sublimation following Pomeroy and Li (2000) described below, and simplified algorithms from Essery *et al.* (1999);
4. Interception: studies rainfall interception based on Rutter *et al.* (1972; 1975), Rutter and Morton (1977), Liu *et al.* (1998) and snowfall interception and sublimation based on Hedstrom and Pomeroy (1998); Pomeroy *et al.* (1998); Parviainen and Pomeroy (2000);
5. Radiation: selects routines for shortwave direct and diffuse algorithms, slope corrections (Garnier and Ohmura, 1970), snow albedo decay (Gray and Landine, 1987), longwave radiation (Sicart *et al.*, 2004), canopy transmissivity (Pomeroy and Dion, 1996) and net radiation (Granger and Gray, 1990);
6. Evaporation: Selection of routines from Penman-Monteith, Granger and Pomeroy (1997), and Shuttleworth and Wallace (1985).
7. Snowmelt: Selects from the Energy Balance Snowmelt Model (Gray and Landine, 1988), fractal snowmelt and snow cover depletion (Shook, 1995), simple land surface scheme style melt model (Essery and Etchevers, 2004); meltwater routing (Albert and Krajeski, 1998), net radiation and temperature index melt (Kustas *et al.*, 1994).
8. Infiltration: uses a variety of infiltration routines for frozen soils, basic method from Granger *et al.* (1984), parametric method from Gray *et al.* (2001), frost depth calculation, simple unfrozen soil infiltration, Green-Ampt infiltration and redistribution (Ogden and Saghafian, 1997),
9. Soil moisture balance: uses multiple flowpath 3 layer linear reservoir model with options for fill and spill, saturation overland flow, shallow subsurface drainage and groundwater drainage.
10. Flow: studies organic layer flow based on conceptual model by Quinton and Marsh (1999), Quinton and Gray (2001) and independent timing and storage control of overland, mineral interflow, groundwater flow and streamflow using the lag and route hydrograph method by Clark (1945).

Some examples of key CRHM modules and their physical basis are provided below; however a complete description of all components and module options currently available in CRHM is beyond the scope of a single journal paper and can be accessed from the CRHM
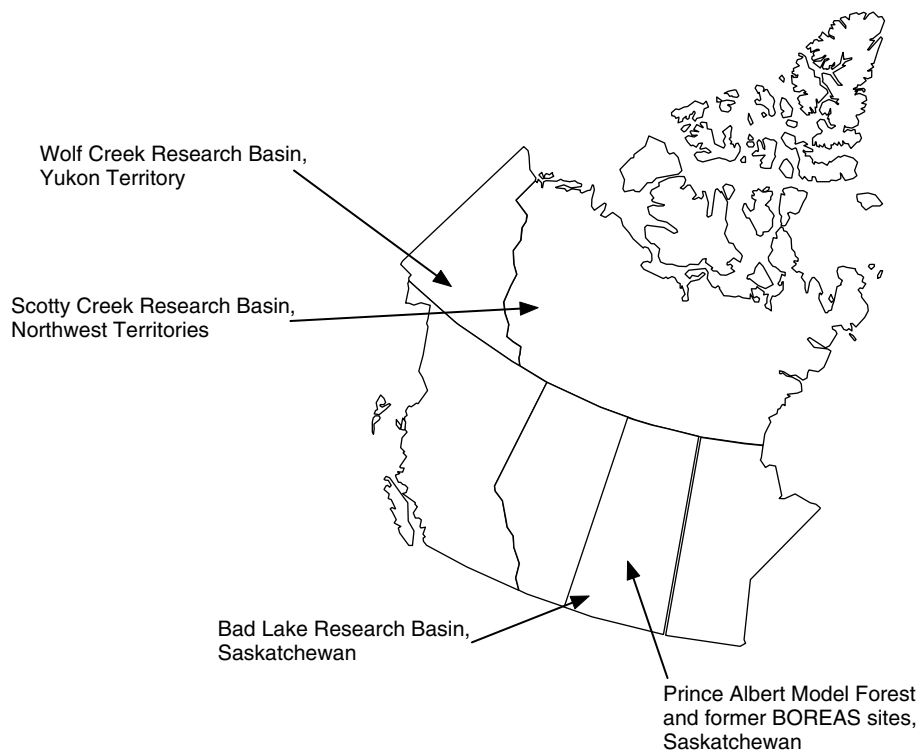
Figure 1. Locations of the research and modeling sites in western Canada. Bad Lake, Saskatchewan: semi-arid prairies, Prince Albert Model Forest/BOREAS, Saskatchewan: southern boreal forest, Wolf Creek, Yukon: sub-arctic cordilleran tundra, Scotty Creek, Northwest Territories: sub-arctic permafrost wetland

website: http://www.usask.ca/hydrology/crhm.htm. The locations where these modules were developed are in western Canada (Figure 1) and are referred to throughout the text.

Prairie blowing snow module

The physics of snow transport and sublimation involve phase change, two-phase flow in saltation and suspension and rapid energy and mass transfers in the atmospheric boundary layer just above the snowpack. Blowing snow on the Canadian prairies was found to be a major transport mechanism for snow, with redistribution causing snow water equivalent (*SWE*) accumulation on various landscape types within a basin to vary from 0·6 to 4·2 of accumulation on a level unvegetated plain (Gray and others, 1979). Transport fluxes from open fields varied from 8 to 36% of snowfall while sublimation in transit converted from 15% to 41% of snowfall to water vapour (Pomeroy and Gray, 1995). Blowing snow was not found to be a significant transport process in either Yukon or Saskatchewan boreal forest environments; however blowing snow is important in alpine sites (Pomeroy *et al.*, 1999).

The prairie blowing snow model (PBSM) was first developed in 1987 as a single column mass and energy balance that calculates blowing snow transport and sublimation rates (Pomeroy, 1989) and later extended to include a snow cover mass balance for the case of two dimensions (Pomeroy *et al.*, 1993) and in recent versions for three dimensions (Essery *et al.*, 1999). The model used in CRHM is a modified, single column calculation

with new methods to calculate the inputs and to scale the fluxes from a point to a landscape in an areal snow mass balance calculation. The snow mass balance on a HRU is the result of the distribution and divergence of blowing snow fluxes surrounding the element and within the element (Pomeroy *et al.*, 1997). The following, upscaled, mass balance can be drawn over an HRU having fetch distance, x (m),

$$\frac{dSWE}{dt}(x) = P - p\left[\nabla F(x) + \frac{\int E_B(x)\,dx}{x}\right] - E - M$$

(1)

where *dSWE/dt* is surface snow accumulation rate (kg m^{-2} s^{-1}), P is snowfall rate (kg m^{-2} s^{-1}), p is the probability of blowing snow occurrence within the HRU, F is the downwind transport rate (kg m^{-1} s^{-1}), E is snow surface sublimation rate (kg m^{-2} s^{-1}), E_B is blowing snow sublimation rate (kg m^{-2} s^{-1}), and M is snow melt rate (kg m^{-2} s^{-1}). Application of the blowing snow algorithms to solve for the snow mass balance requires calculating each term of Equation (1); the fluxes and the control volume assumption are shown in Figure 2.

The PBSM module corrects for Nipher snowfall gauge undercatch and calculates *SWE* accumulation as a residual of snowfall, snow transport and sublimation. It links to snowmelt modules for the other terms. Transport and sublimation of blowing snow are calculated every interval (normally hourly) using the wind speed, air temperature and relative humidity. Snow is redistributed between HRU based on snow transport calculations, and HRU
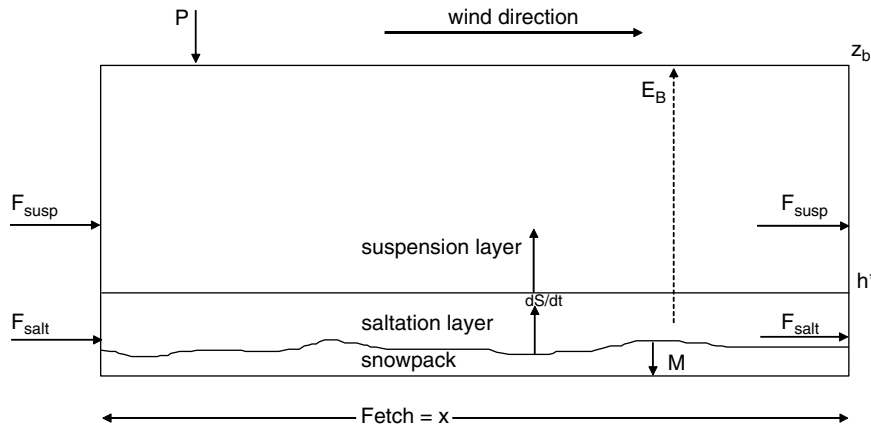
Figure 2. Cross-sectional view of PBSM control volume over an HRU, illustrating Equation (1). Note that the subscripts salt, susp refer to saltation and suspension respectively

dimensions, routing order and a distribution factor. The routing order goes from HRU with the lowest vegetation height to the highest. The distribution factor is entered based on the contact length between HRU and estimates of prevailing wind direction. Essery and Pomeroy (2004) have recently shown that simple systems of source and sink HRU based upon vegetation height can provide similar basin average *SWE* to a fully distributed blowing snow model.

Energy balance snowmelt module

Snowmelt rate along with *SWE* controls the duration and intensity of snowmelt discharge and the delivery of water from snow to the soil and stream in spring. This module is based upon an energy-budget snowmelt model developed for the Canadian prairies with modifications to include the effect of slope and aspect on incoming direct and diffuse shortwave radiation. Melt rates have been found to be highly sensitive to vegetation cover, slope, and aspect as they influence incoming shortwave radiation to the snow surface (Pomeroy and Granger, 1997; Pomeroy *et al.*, 2003). For comparison to the full energy balance calculation there is an option to use the simplified energy budget method proposed by Kustas *et al.* (1994). Snowmelt involves the change of phase of ice to liquid water. Therefore, the energy equation is the physical framework for snowmelt calculations and involves the application of the energy equation to a 'control volume' of snow. The volume has as its lower boundary the snow-ground interface and as its upper boundary the snow-air interface (Figure 3).

The energy budget requires that the amount of energy used for the phase change plus the sum of the fluxes transferred to the volume by radiation, convection, conduction, and advection must equal the change in internal energy. That is:

$$Q_m + Q_n + Q_H + Q_E + Q_G + Q_D = \frac{dU}{dt} \quad (2)$$

where: Q_m is energy available for snowmelt, Q_n is net radiation, Q_H is turbulent flux of sensible heat, Q_E is
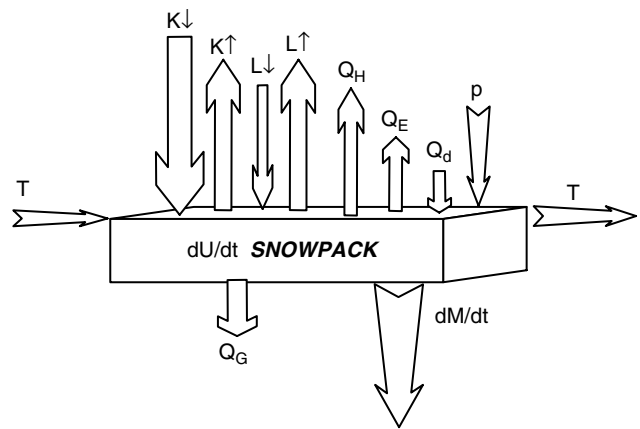

Figure 3. HRU scale control volume for snowmelt calculation. Note that T refers to horizontal transfer of snow mass which can occur due to blowing snow but is infrequent during melt. Arrows indicate direction of fluxes

turbulent flux of latent energy, Q_G is ground heat flux, Q_D is energy due to advection from external sources, such as heat added by falling rain, convective heat derived from the movement of large, warm air masses and heat derived from patches of soil lying adjacent to patches of snow, and dU/dt is the rate of change of internal (stored) energy in the volume per unit surface area per unit time (all unts are W m^{-2}). The fluxes of energy directed towards the control volume are taken as positive; those directed away from the volume are negative. The net radiation, Q_n is composed of the sum of net longwave L^* and net shortwave K^* fluxes. The amount of melt, M, is calculated from Q_m by the expression:

$$M = \frac{Q_m}{\rho_w B \, h_f} \quad (3)$$

in which ρ_w is the density of water (1000 kg m^{-3}), B is the thermal quality of the snow, the fraction of ice in a unit mass of wet snow (B usually ranges between 0·95 and 0·97) and h_f is the latent heat of fusion of ice (333·5 kJ kg^{-1}). When Q_m is in W m^{-2}, daily melt, M (mm day^{-1}) can be approximated as:

$$M = 0.270 \, Q_m \quad (4)$$

Gray and Landine (1988) provide equations for turbulent transfer of sensible and latent heat derived from detailed profile measurements of temperature and humidity along with convective flux observations over melting snow at Bad Lake (Granger and Male, 1978). The net radiation algorithm is derived from equations developed by Brunt (1932), Brutsaert (1982) and Garnier and Ohmura (1970) with local atmospheric coefficients based upon observations at Bad Lake.

Critical to net radiation is estimating the albedo, A(t). Based on several years of point and areal measurements of reflected short-wave radiation during snow ablation, Gray and Landine (1987) divided the seasonal variation in albedo of prairie snowcovered landscapes between 1 February and the end of ablation into three periods:

Premelt—from 1 February up to the start of active melt, albedo decreases at a relatively constant rate, except for event-caused increases due to snowfall and decreases due to melting. Rates of depletion range from 0·004 to 0·009/day with an average of 0·0061/day.

Melt—the general shape of the albedo-depletion curve during continuous melt is 'S'-shaped in which the period of rapid decrease in albedo is preceded and followed by one or two days when the rate of change is slower. The decrease during rapid, continuous melt is approximated by the expression:

$$A(t) = A_i - 0.071t, \qquad (5)$$

in which $A(t)$ is the albedo after 't'-days of continuous depletion and A_i is the albedo of the snow surface at the start of 'active' melt. The period of ablation of shallow arctic and prairie snowcovers under continuous melting often spans only 4 to 7 seven days.

Postmelt—following the disappearance of the seasonal snowcover, the albedo of the ground surface takes on a relatively-constant value of 0·17 (the value can be adjusted). The decrease in albedo of late-occurring snows occurs at the rate of about 0·20/day.

Once slope corrections have been applied to incoming direct and diffuse shortwave radiation and albedo has been calculated, then for the melt period Q_n is calculated as a linear function of the daily net short-wave radiation, Q_o, the albedo, and the sunshine ratio by the expression

$$Q_n = -0.53 + 0.47 \, Q_o \left(0.52 + 0.52 \left(\frac{n}{N}\right)\right) (1 - A(t)) \qquad (6)$$

Equation (6) has a correlation coefficient of 0·87 and a standard error of estimate of 1·55 MJ m^{-2} d^{-1} (Gray and Landine, 1988) The ratio n/N is that of the actual hours to potential hours of bright sunshine. CRHM has an algorithm to estimate n/N from observed incoming shortwave radiation, as 'sunshine hours' are becoming scarce in meteorological records.

Gray and Landine (1988) also presented an algorithm for modelling the internal energy changes on a daily basis in a shallow prairie snowcover using the daily minimum temperature to define the minimum state and assuming a maximum value in internal energy of zero at 0 °C. On days when melt occurs, up to 5% by weight of liquid water can exist within a snowpack. Re-freezing of this water during the evening produces large changes in the internal energy content of a snowcover.

Infiltration to frozen soils module

This module handles frozen soil infiltration (*INF*), during snowmelt and over-winter soil moisture changes. The algorithms are based upon 15 years of study of the snow hydrology of the prairie region of Canada (Gray *et al*., 1986) and results reported in the former USSR (Motovilov, 1978; 1979; Popov, 1973). The Division of Hydrology at the University of Saskatchewan (Granger *et al*. 1984), postulated that the infiltration potential of frozen soils may be grouped in three broad categories, namely: restricted, limited and unlimited.

Restricted—Infiltration is impeded by an impermeable layer, such as an ice lens on the soil surface or within the soil close to the surface. For all practical purposes, the amount of meltwater infiltration can be assumed to be negligible and that the melt goes directly to runoff and a little to evaporation. $INF = 0$.

Limited—Infiltration is governed primarily by the snow-cover water equivalent and the frozen water content of the top 30 cm of soil.

Unlimited—This soil has a high percentage of large, air-filled macropores at time of melt. Examples of soils having these properties are dry, heavily cracked clays and coarse, dry sands. All meltwater infiltrates these soils and runoff from overland flow is negligible. $INF = SWE$.

Granger *et al*. (1984) made field observations in Bad Lake and surrounding farmland of infiltration from snowmelt to medium to fine-textured, uncracked frozen prairie soils in which entry of meltwater is not impeded by ice layers (limited case). The findings show that:

1. the mean depth of infiltration during snowmelt was 260 mm,
2. infiltration was relatively independent of soil texture and land use,
3. the amount of snowmelt infiltration was inversely related to the average moisture content of the 0–30 cm depth soil layer (θ_p) at the time of melt.

These findings are supported by further observations and physical modelling in the Prince Albert Model Forest and Wolf Creek Research Basin boreal and tundra soils (Zhao and Gray, 1999; Gray *et al*., 2001; McCartney *et al*., 2006).

Granger *et al*. (1984) derived a set of equations defining the relationship between total snowmelt infiltration (*INF*, mm) and premelt *SWE* (mm) based on θ_p, where,

$$INF = 5(1 - \theta_p) \, SWE^{0.584} \qquad (7)$$

This equation and the infiltration classification framework described above have been implemented to improve the performance of hydrological models in the prairie environment (Gray *et al.*, 1985; 1986) and the following description of their use in CRHM is based upon this experience.

In CRHM, the user is required to specify the autumn soil moisture content for each HRU as a parameter. These can also be simulated from the previous year's model run. The autumn soil moisture content is used to calculate θ_p and to help determine the infiltration category. When there is an early melt and subsequent re-freezing causing an ice lens to form, both limited and unlimited cases change to restricted. Implementation of the infiltration to frozen soils routine uses the following definitions:

1. The index, I, $= INF/SWE$ where INF is determined using the classification above including Equation (7). and SWE is determined from the blowing snow model
2. The potential, P, $= INF/6$.
3. The melt threshold, M_T, $= 5$ mm. This is the minimum daily meltwater at which the melt routine is enabled. Lower meltwater levels are not counted as one of the six major melt events.
4. A major melt is a day when the meltwater is greater than M_T.
5. Six major daily melts are allowed before the infiltration category is changed to Restricted.

The Frozen Soil Infiltration routine is enabled to start any time after the beginning of November. It is triggered into operation by the first major melt. At this time, I and P are calculated from the soil moisture (θ_p) and the SWE of the snowpack. I and P are recalculated if another major melt occurs with a greater SWE. The Frozen Infiltration routine is disabled when the SWE of the snowpack is less than 5 mm. Disabling the frozen infiltration routine at a SWE of 5 mm is reasonable for shallow snowpacks, which melt.

The following criteria apply to the module:
Limited:

1. Only six major over-winter snowmelt events are possible before the infiltration potential is set to Restricted.
2. Meltwater amounts less than M_T are allowed to infiltrate into the soil using the unfrozen soil infiltration algorithm. Once M_T has been exceeded (normal spring snowmelt) only the amount of meltwater equal to $M \times I$ will infiltrate and the remainder will be handled as runoff. That is, after a major melt the normal fast storage infiltration limits for unfrozen soil are suppressed and the frozen soil routines take over.
3. If the temperature on the day following a major melt event is colder than $-10\,°$C, it is assumed that an ice lens has formed, and the category is changed from Limited to Restricted.

Unlimited:

1. All meltwater is allowed to infiltrate after a major snow melt event. Prior to this, infiltration is handled by the normal infiltration routine.
2. Unlimited is ended when the model returns to its normal infiltration routine at the end of melt.

Restricted:

1. No meltwater is allowed to infiltrate.
2. When SWE is less than 5 mm, the category is no longer applicable as the frozen infiltration routine is no longer operational in the program. The model will thereafter use its normal unfrozen soil infiltration routines.

Evapotranspiration module (Granger and Pomeroy, 1997)

Actual evapotranspiration, $E = Q_E/L_v$, is calculated using the algorithm of Granger and Pomeroy (1997), based on Granger and Gray (1989), which is an extension of the Penman equation to unsaturated conditions under conditions with minimal advection. The latent heat of vapourisation L_v is used with the evaporative heat flux, Q_E, found as

$$Q_E = \frac{G[s\,(Q^* - Q_G) + C\,vdd_a/r_a]}{s\,G + \gamma} \quad (8)$$

where C is the specific heat capacity of air (J kg^{-1} K^{-1}), vdd is vapour density deficit (kg m^{-3}), r_a is aerodynamic resistance (s m^{-1}), s is the slope of the saturation vapour density curve (kg m^{-3} K^{-1}), γ is the psychrometric constant (kg m^{-3} K^{-1}), G is the relative (saturated) evaporation (dimensionless) and D is the relative drying power (dimensionless). The terms G and D are found from:

$$G = 1/(0\cdot793 + 0\cdot2\exp(4\cdot902D)) + 0\cdot006D$$
$$D = \frac{L_v vdd_a/r_a}{(L_v vdd_a/r_a) + Q^* - Q_G} \quad (9)$$

where L_v is the latent heat of vaporization (J kg^{-1}). The aerodynamic resistance is found from wind speed and vegetation roughness height. This algorithm does not require knowledge of soil moisture status, but uses the aridity of the atmosphere to index and ability of soil and vegetation to supply water for evaporation. It has received extensive testing (Granger and Gray, 1989; Granger and Pomeroy, 1997; Carey *et al.*, 2005) and is suited for daily estimates of evapotranspiration.

Evapotranspiration (total calculated by Equation (8) is segregated into evaporation of intercepted rainfall in the canopy, surface evaporation, and transpiration using the equations of Rutter *et al.* (1972) to determine canopy interception and the Green-Ampt module to determine surface infiltration rate (surface storage is available for surface evaporation). Water that has infiltrated to the soil column is deemed to be available for transpiration. The total of transpiration, evaporation from the surface, and

interception evaporation must equal evapotranspiration. To ensure a water balance within HRU and basin, evapotranspiration is halted by CRHM when all available sources of intercepted, surface and soil water are depleted.

Soil moisture balance

This module handles soil moisture accounting for both frozen and unfrozen periods. When snow cover is present, the input to this module is the infiltration (*INF*) generated by the snowmelt infiltration module. From the end of snow melt untill late fall, *INF* is generated by the runoff module. The soil is handled as two layers. The top layer is called the recharge layer and represents the top soil. Evaporation ($E_{SURFACE}$) can only occur from the recharge layer; however water for transpiration (*Trans*) is withdrawn from the entire soil depth. Surface infiltration satisfies the available storage of the recharge layer first before moving to the lower soil layer. Excess water from

both soil layers satisfies the ground water flow (*GW*) before being discharged to the sub-surface flow (*SSR*). Field capacity is specified as a parameter representing the maximum soil moisture (θ) capacity for the two layers. The wilting point (transpiration = 0) is when the state variables soil recharge and soil moisture content are equal to zero.

The mass balance for the soil moisture module is

$$INF - GW - SSR - E_{SURFACE} - Trans - \Delta\theta = 0$$
(10)

The linkages between the soil moisture balance module, and evaporation, infiltration, and interception modules are shown in Figure 4. The infiltration equation is an implementation of the Green-Ampt equation after snowmelt and uses the infiltration to frozen soil routine for snowmelt over frozen ground. Interception is calculated using Rutter's method (Rutter *et al*., 1972; 1975). A routing module handles the
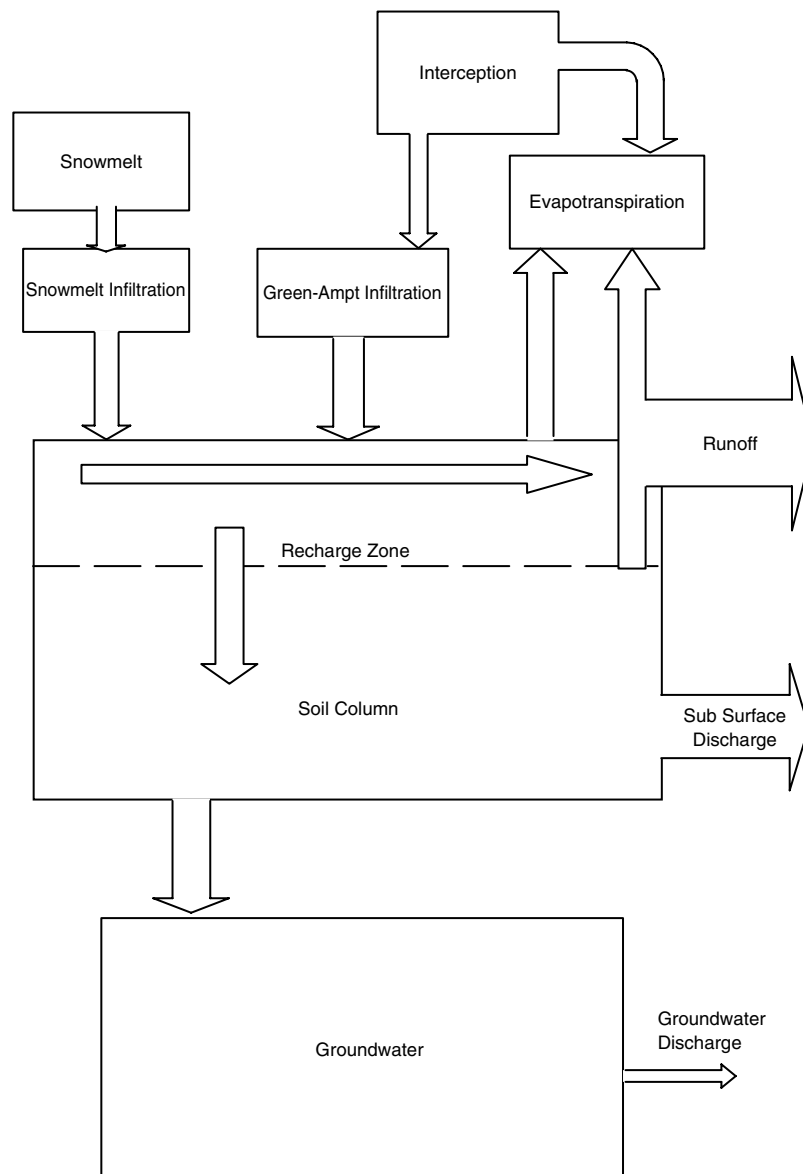

Figure 4. Flows associated with the soil moisture balance module

movement of runoff, subsurface flow and groundwater flow between HRU.

Flow modules

These modules calculate subsurface drainage from hillslopes in organic-covered terrain. Although they were designed for environments where organic soil overlies saturated permafrost, they are also suited for permafrost-free terrains where organic soils overlie other types of relatively impermeable substrates, such as bedrock, dense clay, or transient ice lenses.

Recent field studies in organic-covered, permafrost terrains, including arctic and alpine tundra, taiga, and northern boreal forest and wetland, have demonstrated that lateral flow is the primary pathway affecting water transit time from infiltration into the ground until arrival at the base of hillslopes, as the vertical transit time from the ground surface to the water table is negligible (Quinton and Marsh, 1999; Quinton and Gray, 2001; 2003). Quinton *et al.* (2000) used a hydraulic analysis to demonstrate that lateral flow through the organic soil is laminar and can be described by Darcy's law. These studies formed the basis of a mass transport algorithm, where lateral subsurface runoff from each HRU, is computed from the HRU slope, and the transmission properties of the soils in the saturated layer (Quinton *et al.*, 2004).

Since the frost table is relatively impermeable, the elevation of the saturated layer depends on the degree of soil thaw. The mass flow algorithm was therefore coupled to a heat flow routine in order to estimate subsurface runoff from hillslopes during soil thawing. The cumulative average daily heat flux into the ground ΣQ_g is estimated from its strong linear association with the cumulative average daily ground surface temperature ΣT_s (Quinton and Gray, 2001; 2003). The modules then compute the fraction of ΣQ_g used to lower the frost table ΣQ_i based on the soil thermo-physical properties of the peat matrix at the thawing front. The increase in the depth to the impermeable frost table is then computed by converting ΣQi into the equivalent cumulative depth of thaw dt,

$$\Sigma dt = (\Sigma Q_i / \rho_I h_f) f_i \qquad (11)$$

where Q_i is in units of J m^{-2}, ρ_i is the density of ice, h_f is the latent heat of fusion, and f_i is the volume fraction of ice at the frost table. f_i is equivalent to the porosity, ϕ (i.e. the soil is assumed to be saturated with ice). The association between ΣT_s and ΣQ_g also offers the prospect of using remotely-sensed thermal infra-red imagery to estimate the rate of frost table lowering with time. The user must specify the coefficients in the $\Sigma Ts - \Sigma Q_i$ association, and the initial depth of the top of the frozen, saturated layer (i.e. frost table) at the time that the ground surface becomes snow-free, since it is from that time forward that the cumulative energy input is recorded. Recent field studies by Quinton *et al.* (2004) demonstrated a strong association between the cumulative net all-wave radiation ΣQ_n and ΣQ_i, suggesting that Q_n

could also be used in future versions. The flow modules do not presently compute a temperature distribution in the soil. Instead, the frozen soil is warmed from the user-specified initial temperature to the melting point at 0 °C, and the meltwater produced and recorded for the water balance, is assumed to remain at that temperature.

The modules, as applied to hillslopes, calculate subsurface drainage from a unit width strip, perpendicular to the slope. They require three types of continuous data input: rainfall, air temperature for the snowmelt computation, and ground surface (i.e. skin) temperature for the computation of ground thaw. The modules recognize two types of HRU, a snowpack HRU that provides meltwater drainage, and a snow-free hillslope HRU that conducts and stores the meltwater input in addition to inputs from rainfall and the melt of ice in the active layer. The hillslope HRU requires that the slope gradient, the overall thickness of the soil, and the number of computational layers be defined. For each soil layer, key thermal (i.e. volumetric heat capacity) and physical (i.e. bulk density and porosity, ϕ) properties, and initial soil temperature must be defined. Within each layer, the depth of water (m) held by surface tension may be set as a constant value, or may be calculated from the Van Genuchten (1980) expression. Any excess water is assumed to be available for subsurface drainage. When the soil tension is less than the bubbling pressure, ψ_b, the soil is assumed to drain by gravity, otherwise:

$$\theta_f = (\phi - \theta_r)^*(2^n)^{-m} + \theta_r, \qquad (12)$$

where $\psi_b = 1/\alpha$, θ_f is the soil moisture available for subsurface drainage. Above the bubbling pressure the volumetric soil moisture is

$$\theta = (\phi - \theta_r)^*((1 + (\alpha|\psi|)^n)^{-m} + \theta_r \qquad (13)$$

where θ is the computed volumetric soil moisture content, θ_r is the residual volumetric soil moisture content determined from the moisture-tension characteristic curves, ψ is the soil moisture tension (m) equal to the depth of water standing on the HRU frost table and is equal to the sum of the water available for subsurface drainage of all layers above the frost table, n is a constant, $m = 1 - 1/n$, and $\alpha = a^*m - 1$. Default values for a and n are 25 and 3·0 respectively for above 0·1 m and 15 and 2·2 for greater depths, however other values can be specified by the user.

In addition to the layer properties, the saturated horizontal hydraulic conductivity is defined for the entire organic soil profile. Because in organic soils, the hydraulic conductivity k typically decreases exponentially with depth, the depth variation in k is expressed as

$$k = aNd^{bN} \qquad (14)$$

for which d is the depth to the middle of the thawed saturated layer from the ground surface. Default values are $aN = 0·011$ and $bN = -4·2178$, based on the k-depth (k-d) association defined by Quinton and Gray

(2003), although the user can specify other values. The k-d association enables the user to maintain appropriate values of *k* for the saturated flow zone as the relatively impermeable frost table lowers through the soil profile during ground thawing.

The hillslope HRU can be divided into as many as 100 sub-HRUs in order to accommodate variations in slope gradient. This feature provides a diagnostic tool in that water balances and flow and storage processes can be computed simultaneously for different sections of the hillslope strip. The subsurface drainage water (i.e. excess water) is routed downslope along the user-specified routing order of sub-HRUs using the lag and routing method of Clark (1945) that calculates the outflow from each sub-HRU. Input parameters are a lag time and storage constant for each sub-HRU, or for the single HRU if no sub-HRUs are used. A lag time and storage constant can also be specified for the snowpack HRU in order to route the meltwater wave from the surface to the base of the melting snowpack.

SIMULATIONS OF COLD REGIONS SNOW, WATER BALANCE AND FLOW

A sample of environments with good data availability because of the presence of a research basin was chosen to test CRHM in conditions that span wet to dry, flat to mountainous regions and for seasons from winter to summer. Only open environments were tested as the model is being evaluated in forested environments as part of a snow model intercomparison (Rutter and Essery, 2006). The model was evaluated using observations of SWE, snowmelt, runoff, evaporation, frost table, and streamflow at sites in Saskatchewan, Yukon and the Northwest Territories.

Snow accumulation and melt

Examples of CRHM simulations and measurements of the winter and spring water balance from single HRU open sites in the three research areas are shown in Figure 5 with simulations that use blowing snow
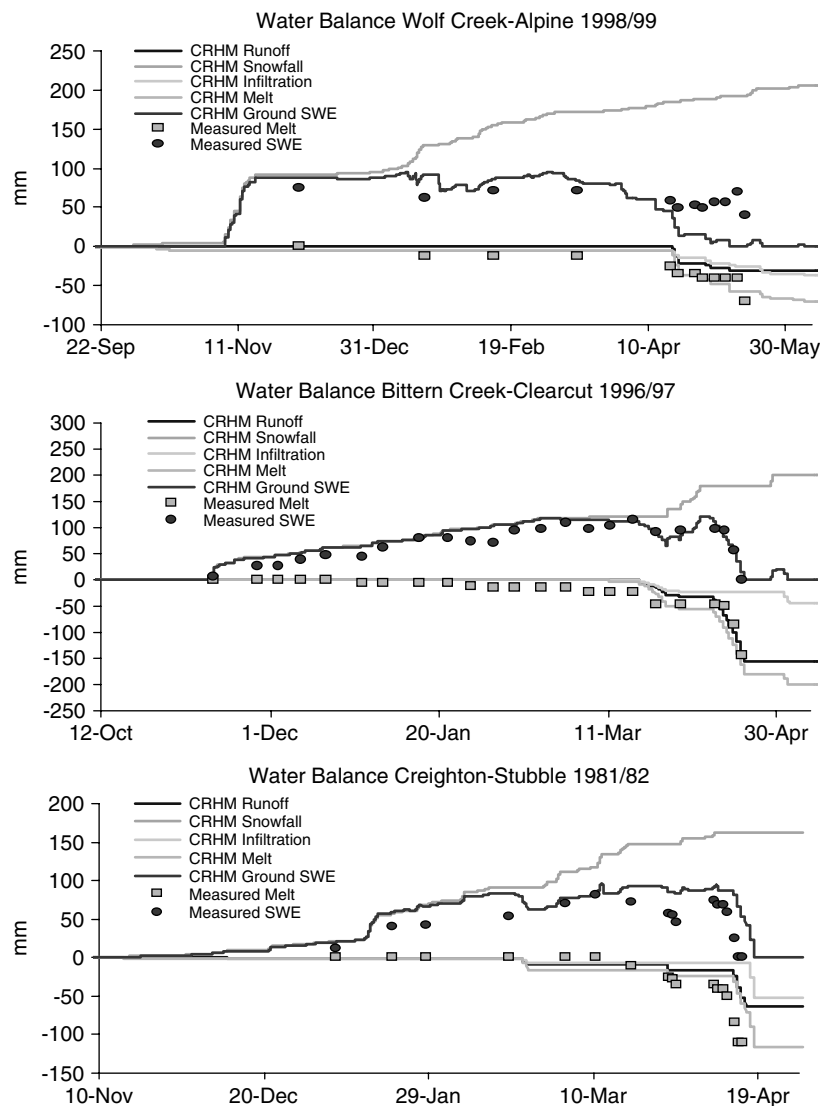

Figure 5. Simulations using the Cold Regions Hydrology Model with modules for energy balance snowmelt, blowing snow, infiltration to frozen soils, and snowmelt runoff for sites in the Prince Albert Model Forest (clear cut, Bittern Creek), Wolf Creek Research Basin (alpine ridge) and Bad Lake Research Basin (Creighton Tributary grain stubble field). Measurements of *SWE* and snowmelt were derived from extensive snow surveys

transport, infiltration to frozen soils, snowmelt, and runoff generation modules. The sites chosen are an alpine ridge top in Wolf Creek, a boreal forest clear cut in the Prince Albert Model Forest and a grain stubble field in Creighton sub-basin of Bad Lake. All sites have a distinct, cold snow-covered winter, with rapid melt in the spring, completely frozen soils at the time of snowmelt and represent environments where spring snowmelt is normally the most important hydrological event of the year. The Wolf Creek alpine site is a sparsely vegetated sub-arctic tundra plateau on a ridge top at 1615 m elevation, with gravely sandy-loam soils overlain by a thin organic layer; the alpine site is characteristic of 20% of the Wolf Creek basin. Bittern Creek is a basin in the Prince Albert Model Forest that has been subject to substantial clear-cutting; the clear-cut site is typical of a recently disturbed site with a chaotic mixture of clay, silt, and sand soils and small shrub and young aspen and conifers less than one metre in height. Clear cuts occupy extensive areas in the southern boreal forest of western Canada where commercial harvesting has taken place. Creighton Tributary flows into Bad Lake and the stubble field represents the most common land use in Saskatchewan grain growing regions and other prairie regions. Soil on the stubble field is light brown and of glacial and lacustrine origin. The simulations are uncalibrated and use measured local parameters for fetch distance, vegetation height, surface albedo, soil properties, and fall soil moisture content. Local meteorological stations were used to provide input variables (wind speed, air temperature, humidity, precipitation, sunshine hours, or incoming solar radiation) for the simulations.

There is reasonable agreement between modelled and measured snow water equivalent accumulation and melt. Differences between measurements and modelled *SWE* at the alpine site in spring are due to difficulties in diagnosing rainfall versus snowfall events (0 °C air temperature was used to divide events and was not adjusted). Similarly the offset in consistently higher *SWE* at the stubble site are likely due to difficulties in diagnosing snowfall versus rainfall in the early winter. The magnitude of over-winter losses of *SWE* to blowing snow underscore the importance of modelling this process in open, snow-covered basins. Modelled melt sequences and quantities are close to observed values and so provide the appropriate inputs for the infiltration and runoff simulations.

The large differences among the winter snow regimes at these sites are due to several factors:

1. The Wolf Creek alpine ridge is extremely windy in the winter and with little vegetation, much of its snowfall is removed by blowing snow.
2. The Bittern Creek clear cut has low winter wind speeds and brush vegetation so there is little to no blowing snow loss.
3. The Creighton stubble field is a windy site, but exposed grain stubble protects snow from wind transport by

partitioning the wind shear force applied to the surface between snow and vegetation.

Despite roughly similar winter snowfall, the spring runoff regimes differ substantially; there was approximately six times greater runoff from the Bittern Creek clear cut than from the alpine ridge in Wolf Creek. In addition to effects due to over-winter wind transport of snowfall, the differences are associated with fall soil moisture status (wetter in the clear-cut) and to the relatively fast melt rates at the stubble and clear-cut sites. As a result runoff and infiltration were roughly equal at the alpine site, runoff was slightly higher than infiltration at the stubble site and runoff greatly exceeded infiltration at the clear-cut site. As these sites do not have streams, it is not possible to verify the runoff estimates at this HRU scale, however the frozen soil infiltration estimates are consistent with observations at these sites (Granger *et al.*, 1984; Pomeroy *et al.*, 1997; Gray *et al.*, 2001).

Small prairie basin runoff

To demonstrate runoff simulations with parameters chosen from basin observations rather than calibration, Creighton Tributary of Bad Lake Research Basin was chosen for a year with near-normal snowfall and good observations of fall soil moisture content, meteorological variables, and streamflow (1974–75). Creighton Tributary had three major land uses in that year; summerfallow (bare field), grain stubble, and native grass, with areas of 3·58, 6·13 and 1·68 km^2 respectively. The basin does not contain large elements of depressional storage so the gross basin area is a close approximation of the contributing drainage area.

CRHM was set up as a 'prairie hydrology model' with the Basin, Observations, Radiation, PBSM, EBSM, frozen infiltration, evaporation, soil moisture balance, and routing (Clark 1945) modules using three HRU corresponding to fallow, stubble, and grass. Parameters were set based on field observations in Bad Lake Research Basin. It was run with hourly observations of air temperature, humidity, wind speed, 6-hourly observations of precipitation, and daily observations of sunshine hours. The simulation of *SWE* and cumulative runoff for the three HRU is shown in Figure 6. Snow accumulation started in early November 1974 and proceeded with no melt until the second week of April 1975. Maximum accumulation of *SWE* in the grass HRU (149 mm) closely matched cumulative snowfall of 154 mm, suggesting that this tall vegetation simply filled in during the winter. Accumulations of *SWE* in the stubble and fallow HRU were significantly reduced at 103 and 59 mm respectively. The model estimated 45 mm of sublimation from blowing snow over the basin; 29% of seasonal snowfall. The runoff ratio (runoff/*SWE*) for the grass HRU was 0·99, reflecting its position near the stream and downslope from other melting surfaces. Runoff ratios for stubble and fallow were much smaller at 0·68 and 0·54 respectively. Note that the model generated no further runoff after
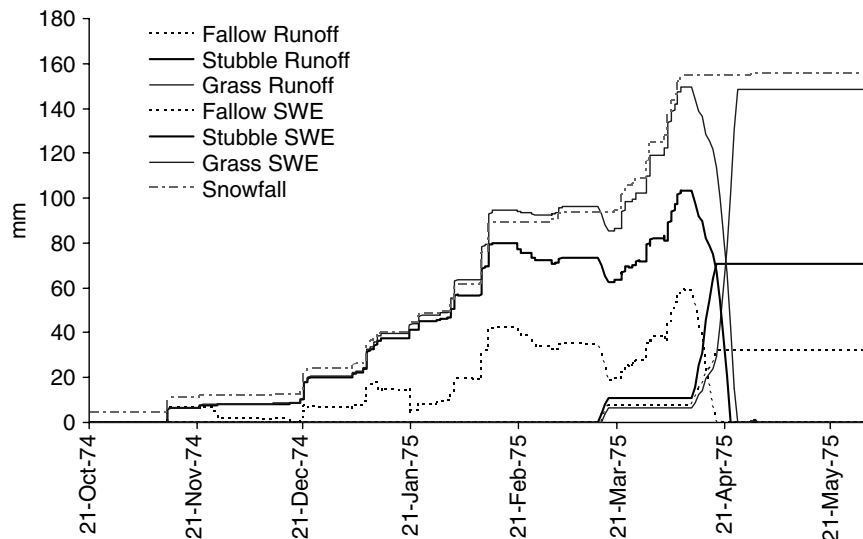
Figure 6. CRHM 'prairie' simulated *SWE* and runoff as mm per unit area for 3 HRU. Corrected cumulative snowfall shown for comparison. Creighton Tributary, Bad Lake, Saskatchewan

spring melt, despite seven rainfall events from late April to late May totalling more than 5 mm per day. The difference is the use of the unfrozen soil infiltration routine after snowmelt.

Figures 7 and 8 show the modelled and observed basin streamflow as a discharge rate (Figure 7) and as cumulative volume (Figure 8). The comparison of rates shows that the model captured both an early and the main runoff event but underestimated the peak flow rate by a factor of three to four and overestimated the duration of streamflow by a factor of two. It is felt that with a more sophisticated routing routine and/or calibration of routing parameters a better fit of the hydrograph could be achieved than with the rather arbitrary storage constant and lag delay parameters that were used. The comparison of cumulative volume in Figure 8 is more promising with the flow volumes being very similar (1038513 m^3 modelled versus 1025398 m^3 observed; ~1% difference), however the shape of the cumulative flow curves are different with the observed being a much sharper rise.

Boreal wetland evaporation

An evaluation of the evaporation, interception, and soil moisture balance modules was conducted at an open fen site in the former BOREAS study area from the beginning of May until the end of October 2004. Observations of evaporation were made in two ways, the first by an eddy correlation system (Campbell CSAT sonic anemometer and LI7500 hygrometer, with axis and other corrections by Fluxnet Canada protocols), and the second by energy balance from the net radiation, less sensible heat (estimated by profile method), and heat storage change. The results are shown in Figure 9 and suggest a good correspondence between evaporation calculated using the Granger-Gray algorithm with an albedo set to 0·1 and to both eddy correlation and energy balance estimates of evaporation. Interestingly, in spring and early summer evaporation is limited by available moisture (cumulative evaporation is roughly equal to cumulative rainfall), whilst in later summer and fall it is no longer limited by precipitation but by energy supply.
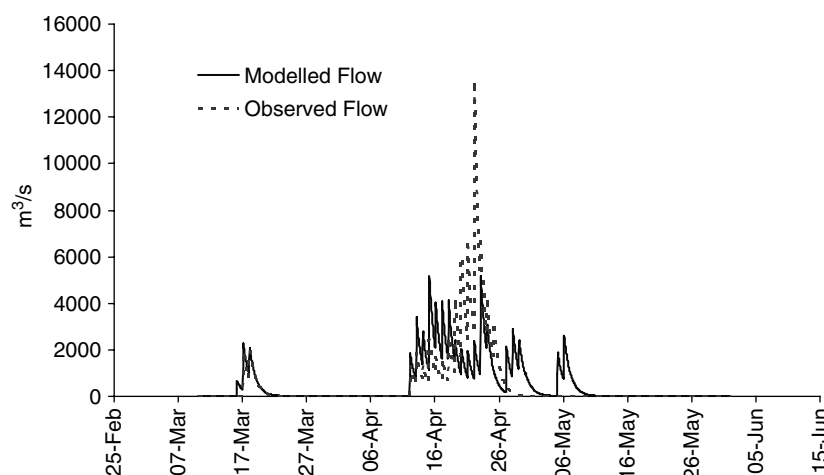

Figure 7. Hourly discharge rate in Creighton Tributary modelled by CRHM and measured, spring 1975
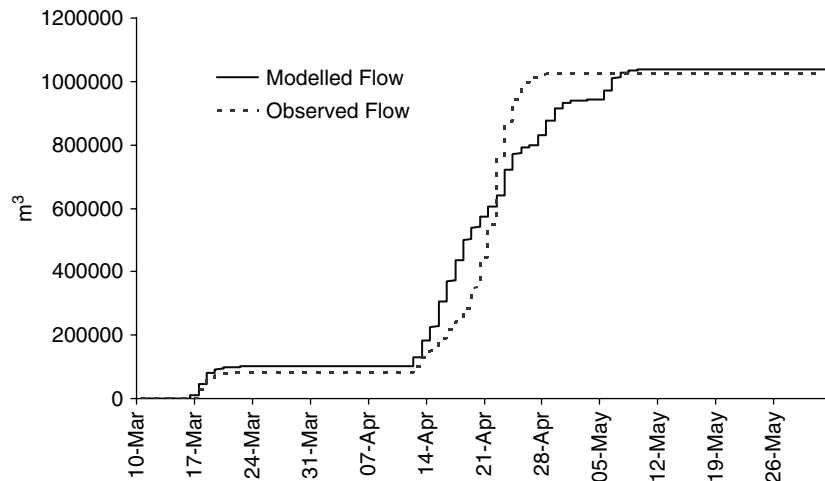
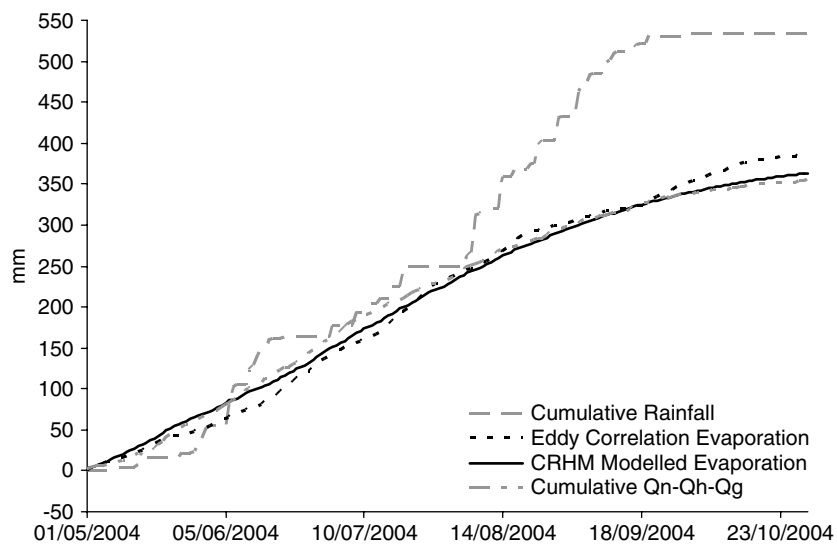Figure 8. Cumulative measured and CRHM-modelled stream discharge, Creighton Tributary (1975)

Figure 9. Modelled cumulative evapotranspiration over a fen wetland in the boreal forest of central Saskatchewan from CRHM and evaporation estimated from eddy correlation measurements and as a residual of the energy balance. Also shown is cumulative rainfall in mm

Tundra hillslope flow

The flow modules were recently tested at two, contrasting cold regions site types: (i) Granger basin, a sub-basin of Wolf Creek, Yukon; and (ii) Scotty Creek, Northwest Territories. At both sites, careful measurements of the water table, frost table, snowmelt, rainfall and soil properties were made in order to initialie and run the flow modules. All computations were made on a 30-min time step.

At Granger basin, field measurement and modelling focussed on a relatively steep ($\sim$0·35), north-facing alpine-tundra hillslope with a late-lying snow drift, and underlain by permafrost. For modelling, the hillslope HRU was divided into seven sub-HRU slope segments, arranged in a strip of unit width normal to the stream channel, as depicted in Figure 10(a). On this slope, the snow cover was dominated by a late-lying snow drift, so the non-drift snowcover was not represented. The triangular cross-section of the snow drift was maintained during ablation following the observed areal depletion

of the drift (Quinton *et al.*, 2004). The soil properties specified in the flow modules were measured at an instrumented soil pit located mid-way between the base and the crest of the slope. At the pit, the organic soil was 0.35 m thick, and contained an upper 0.15 m thick layer of living and lightly decomposed vegetation, overlying a 0.2 m thick layer of relatively dense, humified peat, overlying mineral sediment. In the flow modules, the 0·35 m organic accumulation was divided into three computational layers: a 0·15-m upper layer overlying two 0·1-m thick layers.

At Scotty Creek, modelling focussed on the flank of a 40-m wide peat plateau. In this wetland-dominated region, peat plateaus support a tree canopy, are underlain by permafrost, and are surrounded by channel fens and flat bogs that are open and without permafrost. Unlike the Granger basin study, only a single hillslope HRU was used. Its length was set at 30 m, the distance from the crest to the edge of the peat plateau, over which the slope angle is $\sim$0·01. The use of a single hillslope
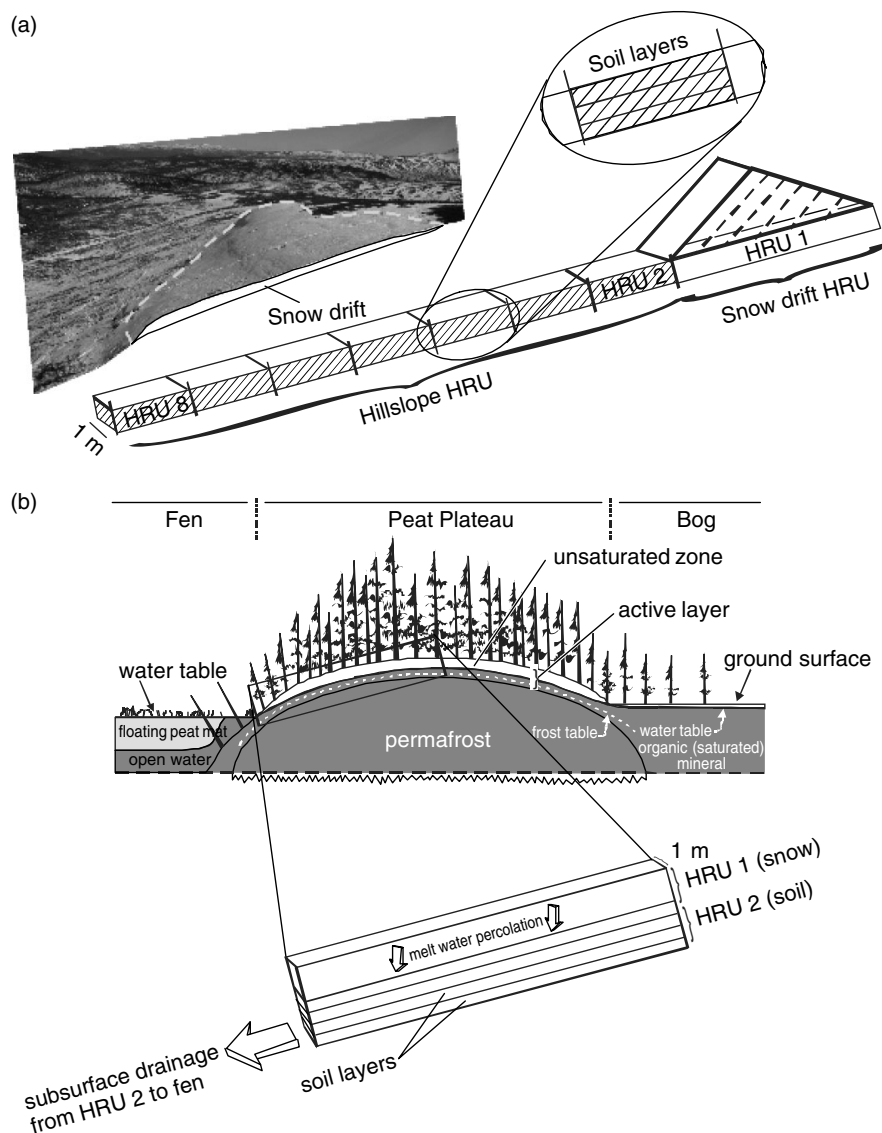
(a)

(b)

Figure 10. Contrasting configurations of HRUs for (a) the Wolf Creek Research Basin where a late-lying snowdrift is situated upslope of a series of hillslope sub-HRUs; and (b) the Scotty Creek Research Basin where peat plateau is covered by a single hillslope HRU resting below a snowpack HRU

HRU removes the need to route water through a series of sub-HRUs, and therefore enables the user to treat the hillslope HRU as though the snowcover HRU is directly above, rather than upslope of the hillslope HRU (Figure 10(b)). As with the Granger basin study, the soil properties specified in the flow modules were measured at an instrumented soil pit located mid-way between the base and the crest of the plateau. However, the soil profile at Scotty was organic throughout the depth of the 0·7 m active layer. The upper 0·15 m was composed of living and lightly decomposed vegetation, while the remainder of the profile contained relatively dense, well humified peat. For the flow modules, four computational layers were defined: 0–0·15 m, 0·15–0·25 m, 0·25–0·35 m, and 0·35–0·70 m.

Simulations for Granger basin suggest that the variation in water table depth between the upper (HRU 2) and lower (HRU 8) regions of the hillslope was minimal while the snow drift was present, and that substantial variations

in water table depth did not develop until mid-June, after the drift had disappeared and the frequency of rainfall increased. The computed rate of melt water release from the drift is plotted with the resulting subsurface drainage from the HRUs at the top (HRU 2) and bottom (HRU 8) of the hillslope in Figure 11(a) for 2002. The 2·75-day time delay between the computed discharge peaks of HRU 2 (27 May at 02 : 00) and HRU 8 (29 May at 20 : 00), suggests that water moved through the 70 m hillslope at an average rate of 25·5 m day^{-1}. This compares closely with the average subsurface runoff velocity derived from the analysis of the continuous radiation and water level records at this site (28·9 m day^{-1}). Given that the portion of the melt period from 19 May to 29 May was characterized by a high level of meltwater input at the top of the hillslope and a high stage level measured in the stream channel at the bottom of the slope, the computed high level of discharge through the intervening hillslope during this period seems reasonable. Although the flow
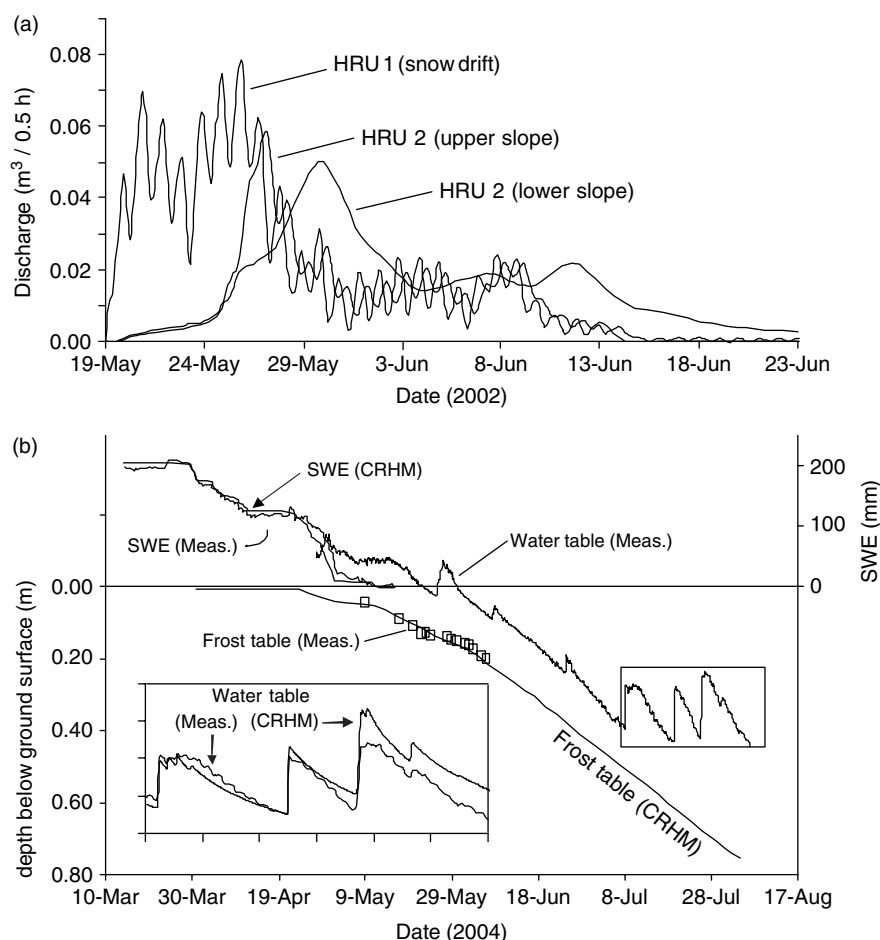
Figure 11. (a) Simulated downslope discharge from upper to lower slope positions of the hillslope HRU during the snowmelt-runoff event of 2002, north-facing slope of Granger Creek, Wolf Creek Research Basin. (b) Measured and simulated snow water equivalent depth, and depth to the frost table and water table at Scotty Creek during the snowmelt-runoff event of 2004

modules seem to provide a reasonable estimate of the measured water table position, Figure 11(b) indicates that this agreement diminishes with time, and is especially noted following large, successive input events. In this instance, the flow modules serve as a diagnostic tool by identifying the need for further research aimed at improving the understanding and representation of the non-linear flow and storage processes characteristic of organic soils.

CONCLUSIONS

Based on process studies in cold regions basins, improvements in the description of snow redistribution, snow interception, snow sublimation, snowmelt, infiltration to frozen soils, evaporation, and tundra hillslope runoff generation were made. These process descriptions have been mathematically described in a physically-based manner and compiled in the object-oriented CRHM, for spatially distributed application to basin prediction.

CRHM has shown some success in multi-objective simulations without calibration of parameters and can model both cold regions and temperate climate hydrological processes. The modules to transfer mass as blowing snow, overland flow, subsurface flow, groundwater flow and streamflow gives the model the ability to simulate

the hydrological cycle in a wide range of environments. For Canadian environments the ability to simulate snow accumulation and redistribution by wind and forest canopies, snowmelt using the energy balance, infiltration into frozen ground and actual evaporation is crucial for understanding the hydrological cycle. Good simulations have been demonstrated for blowing snow redistribution, meltwater infiltration to frozen soils and runoff generation in alpine tundra, forest clearcuts, stubble fields and mixed land use prairie basins. Evaporation routines have been verified in boreal forest open and forest landscapes. Runoff routines have been evaluated in sub-arctic peatlands, permafrost underlain tundra hillslopes and agricultural basins. Some of this success is attributed to CRHM's flexible model structure, strong physical basis, knowledge of local parameters and robust component algorithms. These features permit the incorporation of basin and regional knowledge into model structure and parameter selection and reduce reliance on calibration against streamflow. The combination of targeted field observations and uncalibrated physically-based model diagnosis can provide for rapid advances in the understanding of hydrological systems and is recommended for the transfer of scientific understanding to ungauged or poorly gauged basins where calibration is not normally possible.

The model is well suited for testing the results of new research by developing modules to run in combination with established process modules to provide comprehensive hydrological simulations. Current efforts are to use it to combine inductive and deductive approaches to modelling (Dornes *et al.*, 2006), link it to land surface schemes to provide a flexible modelling test bed for incorporation of hydrological processes in atmospheric models, to add water quality modules, to enhance flow modules (Quinton *et al.*, 2004), to fully test forest modules in a snow model intercomparison experiment (Rutter and Essery, 2006), to model ungauged basins with minimal calibration and to use it to evaluate drought, land use and climate change with physically based modelling (Fang and Pomeroy, 2007). Other researchers are encouraged to use CRHM as a modelling platform—the model is freely available to download, use and modify as a community model for cold regions http://www.usask.ca/hydrology/crhm.htm.

REFERENCES

Abbott MB, Bathurst JC, Cunge JA, O'Connell PE, Rasmussen J. 1986. Introduction to the European hydrological system—Systeme Hydrologique Europeen, 'SHE', 2: structure of a physically-based, distributed modelling system. *Journal of Hydrology* **87**(1–2): 61–77.

Albert MR, Krajeski G. 1998. A fast, physically-based point snow melt model for use in distributed applications. *Hydrological Processes* **12**: 1809–1824.

Bowling LC, Pomeroy JW, Lettenmaier DP. 2004. Parameterisation of the sublimation of blowing snow in a macroscale hydrology model. *Journal of Hydrometeorology* **5**: 745–762.

Brunt D. 1932. Notes on the radiation in the atmosphere. *Quarterly Journal of the Royal Meteorological Society* **58**: 389–420.

Brutsaert W. 1982. *Evaporation into the Atmosphere*. D. Reidel Publishing Company: London.

Carey SK, Barbour SL, Hendry MJ. 2005. Evaporation from a waste rock surface, Key Lake, Saskatchewan. *Canadian Geotechnical Journal* **42**: 1189–1199.

Clark CO. 1945. Storage and the unit hydrograph. *Proceedings of the American Society of Civil Engineering* **69**: 1419–1447.

Dornes PF, Pomeroy JW, Pietroniro A, Carey SK, Quinton WL. 2006. The use of inductive and deductive reasoning to model snowmelt runoff from northern mountain catchments. In *Proceedings of the iEMSs Third Biennial Meeting: "Summit on Environmental Modelling and Software"*, Voinov A, Jakeman AJ, Rizzoli AE (eds). International Environmental Modelling and Software Society: Burlington, USA, Internet: http://www.iemss.org/iemss2006/sessions/all.html. July 2006. CD ROM.

Essery R, Etchevers P. 2004. Parameter sensitivity in simulations of snowmelt. *Journal of Geophysical Research* **109**(D20111): Doi:10·1029/2004JD005036.

Essery RLH, Pomeroy JW. 2004. Vegetation and topographic control of wind-blown snow distributions in distributed and aggregated simulations. *Journal of Hydrometeorology* **5**: 735–744.

Essery R, Li L, Pomeroy JW. 1999. Blowing snow fluxes over complex terrain. *Hydrological Processes* **13**: 2423–2438.

Fang X, Pomeroy JW. 2007. Snowmelt runoff sensitivity analysis to drought on the Canadian prairies. *Hydrological Processes* **21**(19): 2594–2609. DOI: 10.1002/hyp.6796.

Garnier BJ, Ohmura A. 1970. The evaluation of surface variations in solar radiation income. *Solar Energy* **13**: 21–34.

Granger RJ, Gray DM. 1989. Evaporation from natural non-saturated surfaces. *Journal of Hydrology* **111**: 21–29.

Granger RJ, Gray DM. 1990. A net radiation model for calculating daily snowmelt in open environments. *Nordic Hydrology* **21**: 217–234.

Granger RJ, Male DH. 1978. Melting of a prairie snowpack. *Journal of Applied Meteorology* **17**(2): 1833–1842.

Granger RJ, Pomeroy JW. 1997. Sustainability of the western Canadian boreal forest under changing hydrological conditions—2-summer energy and water use. In *Sustainability of Water Resources under Increasing Uncertainty*, Rosjberg D, Boutayeb N, Gustard A, Kundzewicz Z, Rasmussen P (eds). IAHS Publ No. 240. IAHS Press: Wallingford; 243–250.

Granger RJ, Gray DM, Dyck GE. 1984. Snowmelt infiltration to frozen prairie soils. *Canadian Journal of Earth Sciences* **21**(6): 669–677.

Gray DM. 1970. *Handbook on the Principles of Hydrology*. Water Information Center, Inc.: Port Washington, NY.

Gray DM, Granger RJ. 1986. In situ measurements of moisture and salt movement in freezing soils. *Canadian Journal of Earth Sciences* **23**(5): 696 704.

Gray DM, Landine PG. 1987. Albedo model for shallow prairie snowcovers. *Canadian Journal of Earth Sciences* **24**(9): 1760–1768.

Gray DM, Landine PG. 1988. An energy-budget snowmelt model for the Canadian prairies. *Canadian Journal of Earth Sciences* **25**(9): 1292–1303.

Gray DM and others. 1979. Snow accumulation and distribution. In, *Proceedings, Modelling Snowcover Runoff*, Colbeck SC, Ray M (eds). US Army Cold Regions Research and Engineering Laboratory: Hanover, NH; 3–33.

Gray DM, Landine PG, Granger RJ. 1985. Simulating infiltration into frozen prairie soils in streamflow models. *Canadian Journal of Earth Sciences* **22**(3): 464–472.

Gray DM, Granger RJ, Landine PG. 1986. Modelling snowmelt infiltration and runoff in a prairie environment. In *Cold Regions Hydrology Symposium*, Kane DL (ed.) American Water Resources Association: Fairbanks, AK; 427–438.

Gray DM, Toth B, Pomeroy JW, Zhao L, Granger RJ. 2001. Estimating areal snowmelt infiltration into frozen soils. *Hydrological Processes* **15**: 3095–3111.

Hedstrom NR, Pomeroy JW. 1998. Measurements and modelling of snow interception in the boreal forest. *Hydrological Processes* **12**: 1611–1625.

Kite GW. 1995. The SLURP model. In: *Computer models of watershed hydrology*, Singh VP (ed). Water Resources Publications: Colorado, USA; 521–562.

Kouwen N, Soulis ED, Pietroniro A, Donald J, Harrington RA. 1993. Grouping response units for distributed hydrologic modelling. *American Society of Civil Engineers Journal of Water Resources Management and Planning* **119**(3): 289–305.

Kuchment LS, Demidov VN, Motovilov YG. 1983. *River Runoff Formation (Physically Based Models)*. Nauka: Moscow (in Russian).

Kuchment LS, Gelfan AN, Demidov VN. 2000. A distributed model of runoff generation in the permafrost regions. *Journal of Hydrology* **240**: 1–22.

Kustas WP, Rango A, Uijlenhoet R. 1994. A simple energy budget algorithm for the snowmelt runoff model. *Water Resources Research* **30**(5): 1515–1527.

Leavesley GH, Markstrom SL, Restrepo PJ, Viger RJ. 2002. A modular approach to addressing model design, scale, and parameter estimation issues in distributed hydrological modelling. *Hydrological Processes* **16**(2): 173–187.

Leavesley GH, Restrepo PJ, Markstrom SL, Dixon M, Stannard LG. 1996. The Modular Modeling System (MMS) : User's Manual, Open-File Report 96–151, U.S. Geological Survey.

Liu S, Riekerk H, Gholz HL. 1998. Simulation of evapotranspiration from Florida pine flatwoods. *Ecological Modelling* **114**(1): 19–34.

Male DH, Gray DM. 1981. Snowcover ablation and runoff. In *Handbook of snow: principles, processes, management and use*, Gray DM, Male DH (eds). Pergamon Press: Toronto; 776.

McCartney SE, Carey SK, Pomeroy JW. 2006. Intra-basin variability of snowmelt water balance calculations in a subarctic catchment. *Hydrological Processes* **20**: 1001–10016.

Motovilov YG. 1978. Mathematical model of water infiltration into frozen soils. *Soviet Hydrology* **17**(2): 62–66.

Motovilov YG. 1979. Simulation of meltwater losses through infiltration into soil. *Soviet Hydrology* **18**(3): 217–221.

Ogden FL, Saghafian B. 1997. Green and Ampt infiltration with redistribution. *Journal of Irrigation and Drainage Engineering* **123**(5): 386–393.

Parviainen J, Pomeroy JW. 2000. Multiple-scale modelling of forest snow sublimation: initial findings. *Hydrological Processes* **14**: 2669–2681.

Pomeroy JW. 1989. A process-based model of snow drifting. *Annals of Glaciology* **13**: 237–240.

Pomeroy JW, Schmidt RA. 1993. The use of fractal geometry in modelling intercepted snow accumulation and sublimation. *Proceedings of the Eastern Snow Conference* **50**: 1–10.

Pomeroy JW, Gray DM. 1995. *Snow Accumulation, Relocation and Management*, National Hydrology Research Institute Science Report No. 7. Environment Canada: Saskatoon; 144.

Pomeroy JW, Dion K. 1996. Winter radiation exctinction and reflection in a boreal pine canopy: measurements and modelling. *Hydrological Processes* **10**: 1591–1608.

Pomeroy JW, Granger RJ. 1997. Sustainability of the western Canadian boreal forest under changing hydrological conditions—I-snow accumulation and ablation. In *Sustainability of Water Resources under Increasing Uncertainty*, Rosjberg D, Boutayeb N, Gustard A, Kundzewicz Z, Rasmussen P (eds). IAHS Publ No. 240. IAHS Press: Wallingford; 237–242.

Pomeroy JW, Li L. 2000. Prairie and Arctic areal snow cover mass balance using a blowing snow model. *Journal of Geophysical Research* **105**(D21): 26619–26634.

Pomeroy JW, Gray DM, Landine PG. 1993. The prairie blowing snow model: characteristics, validation, operation. *Journal of Hydrology* **144**: 165–192.

Pomeroy JW, Marsh P, Gray DM. 1997. Application of a distributed blowing snow model to the Arctic. *Hydrological Processes* **11**: 1451–1464.

Pomeroy JW, Hedstrom N, Parviainen J. 1999. The snow mass balance of Wolf Creek. In *Wolf Creek Research Basin: Hydrology, Ecology, Environment*, Pomeroy J, Granger R.(eds). National Water Research Institute. Minister of Environment: Saskatoon; 15–30.

Pomeroy JW, Parviainen J, Hedstrom N, Gray DM. 1998. Coupled modelling of forest snow interception and sublimation. *Hydrological Processes* **12**: 2317–2337.

Pomeroy JW, Granger RJ, Pietroniro A, Elliott JE, Toth B, Hedstrom N. 1997. Hydrological Pathways in the Prince Albert Model Forest: Final Report. NHRI Contribution Series No. CS-97007. 153 plus append.

Pomeroy JW, Toth B, Granger RJ, Hedstrom NR, Essery RLH. 2003. Variation in surface energetics during snowmelt in complex terrain. *Journal of Hydrometeorology* **4**(4): 702–716.

Popov EG. 1973. Snowmelt runoff forecasts—theoretical problems. *The Role of Snow and Ice in Hydrology*. UNESCO-WMO-IAHS. Vol. 2. 829–839.

Quinton WL, Marsh P. 1999. A conceptual framework for runoff generation in a permafrost environment. *Hydrological Processes* **13**: 2563–2581.

Quinton WL, Gray DM. 2001. Toward modelling seasonal thaw and subsurface runoff in arctic tundra environments. In *Soil Vegetation, Atmosphere Transfer (SVAT) Schemes and Large Scale Hydrological Models*, Dolman AJ, Hall AJ, Kavvas ML, Oki T, Pomeroy JW (eds). IAHS Publication No. 270. IAHS Press: Wallingford; 333–341.

Quinton WL, Gray DM. 2003. Subsurface drainage from organic soils in permafrost terrain: the major factors to be represented in a runoff model. *Proceedings of the 8th international conference on permafrost*, Davos, Switzerland. 6.

Quinton WL, Gray DM, Marsh P. 2000. Subsurface drainage from hummock-covered hillslopes in the Arctic-tundra. *Journal of Hydrology* **237**: 113–125.

Quinton WL, Carey SK, Goeller NT. 2004. Snowmelt runoff from northern alpine tundra hillslopes: major processes and methods of simulation. *Hydrology and Earth System Sciences Journal* **8**(5): 877–890.

Rutter AJ, Morton AJ. 1977. A predictive model of rainfall interception in forests, III. Sensitivity of the model to stand parameters and meteorological variables. *Journal of Applied Ecology* **14**: 567–588.

Rutter N, Essery RLH. 2006. Evaluation of forest snow processes models (SnowMIP2),. *Geophysical Research Abstracts* **8**: 05921.

Rutter AJ, Morton AJ, Robins PC. 1975. A predictive model of rainfall interception in forests, II. Generalization of the model and comparison with observations in some coniferous and hardwood stands. *Journal of Applied Ecology* **12**: 367–380.

Rutter AJ, Kershaw KA, Robins PC, Morton AJ. 1972. A predictive model of rainfall interception in forests, I. Deriviation of the model from observations in a plantation of Corsican Pine. *Agricultural Meteorology* **9**: 367–384.

Serreze M, Walsh JE, Chapin FS, Osterkamp T, Dyurgerov M, Romanovsky V, Oechel WC, Morison J, Zhang T, Barry RG. 2000. Observational evidence of recent change in the northern high-latitude environment. *Climate Change* **46**: 159–207.

Shook K. 1995. Simulation of ablation of prairie snowcovers. PhD thesis, University of Saskatchewan, 189.

Shuttleworth WJ, Wallace JS. 1985. Evaporation from sparse crops-an energy combination theory. *Quarterly Journal of the Royal Meteorological Society* **111**(469): 839–855.

Sicart JE, Pomeroy JW, Essery RLH, Hardy JE, Link T, Marks D. 2004. A sensitivity study of daytime net radiation during snowmelt to forest canopy and atmospheric conditions. *Journal of Hydrometeorology* **5**: 744–784.

Sivapalan M, Takeuchi K, Franks S, Gupta V, Karambiri H, Lakshmi V, Liang X, McDonnell J, Mendiondo E, O'Connell P, Oki T, Pomeroy JW, Schertzer D, Uhlenbrook S, Zehe E. 2003. IAHS decade on predictions in ungauged basins (PUB), 2003–2012: shaping an exciting future for the hydrological sciences. *Hydrological Sciences Journal* **48**(6): 857–880.

Van Genuchten MT. 1980. A closed form equation for predicting the hydraulic conductivity of unsaturated soils. *Soil Science Society of America Journal* **44**: 892–898.

Woo M-K, Thorne R. 2006. Snowmelt contribution to discharge from a large mountainous catchment in subarctic Canada. *Hydrological Processes* **20**: 2129–2139.

Zhang Z, Kane DL, Hinzman LD. 2000. Development and application of a spatially-distributed Arctic hydrological and thermal process model (ARHYTHM). *Hydrological Processes* **14**: 1017–1044.

Zhao L, Gray DM. 1999. Estimating snowmelt infiltration into frozen soils. *Hydrological Processes* **13**: 1827–1842.